RETINAL DISEASE

IL-18 Attenuates Experimental Choroidal Neovascularization as a Potential Therapy for Wet Age-Related Macular Degeneration

Sarah L. Doyle,[1,2]* Ema Ozaki,[3] Kiva Brennan,[4] Marian M. Humphries,[3] Kelly Mulfaul,[1,2] James Keaney,[3] Paul F. Kenna,[3,5] Arvydas Maminishkis,[6] Anna-Sophia Kiang,[3] Sean P. Saunders,[7] Emily Hams,[7] Ed C. Lavelle,[4] Clair Gardiner,[4] Padraic G. Fallon,[7] Peter Adamson,[8] Peter Humphries,[3] Matthew Campbell[3]*

Age-related macular degeneration (AMD) is the most common form of central retinal blindness globally. Distinct processes of the innate immune system, specifically activation of the NLRP3 inflammasome, have been shown to play a central role in the development of both "dry" and neovascular ("wet") forms of the disease. We show that the inflammatory cytokine interleukin-18 (IL-18) can regulate choroidal neovascularization formation in mice. We observed that exogenous administration of mature recombinant IL-18 has no effect on retinal pigment epithelial (RPE) cell viability, but that overexpression of pro–IL-18 or pro–IL-1β alone can cause RPE cell swelling and subsequent atrophy, a process that can be inhibited by the promotion of autophagy. A direct comparison of local and systemic administration of mature recombinant IL-18 with current anti-VEGF (vascular endothelial growth factor)–based therapeutic strategies shows that IL-18 treatment works effectively alone and more effectively in combination with anti-VEGF therapy and represents a novel therapeutic strategy for the treatment of wet AMD.

INTRODUCTION

Age-related macular degeneration (AMD) is the leading cause of central vision loss in developed countries, affecting 1 in 10 people older than 50 years (http://www.amdalliance.org). With a global increase in the aging population, concurrent with improved life expectancy, the numbers suffering with this progressive, late-onset disease are predicted to increase in 2050 by 50% (*1*). AMD is a complex disease, and a comprehensive understanding of its pathogenesis remains incomplete; however, it is strongly associated with chronic oxidative stress and inflammation.

The inflammatory response in the mammalian system is triggered when microbes or toxins are identified by pattern recognition receptors (*2*), which can induce proinflammatory gene expression (*3*) or lead to the formation of multiprotein platforms known as inflammasomes (*4*). Inflammasomes control the maturation of two major proinflammatory cytokines, interleukin-1β (IL-1β) and IL-18, by allowing for their cleavage from inactive precursors into mature cytokines. Aberrant "sterile" inflammation—inflammation in the absence of infection—is believed to be at the center of a range of age-related disease and occurs when host-derived elements are modified and/or accumulate to form deposits that are not easily cleared.

Early AMD can progress to two late forms of disease: advanced "dry," characterized by the death of underlying retinal pigment epithelium (RPE) and cone photoreceptor cells, or exudative "wet" AMD, characterized by pathological neovascularization of the choroid [choroidal neovascularization (CNV)]. In wet AMD, new blood vessels break through Bruch's membrane/RPE and hemorrhage, causing a blood clot to form between the RPE and foveal cone photoreceptors, resulting in immediate central retinal blindness. About 10 to 15% of individuals with dry AMD will progress to the wet form; yet, it is this minority form of the disease that accounts for almost 90% of the blindness caused by the condition (*5*).

Current antibody-based therapies for AMD target advanced end stages of the disease by inhibiting the activity of vascular endothelial growth factor (VEGF) (*6*). Although this is the only form of effective therapy for AMD currently in use clinically, its use requires direct and regular intraocular injection of monoclonal antibodies (Lucentis, Avastin, or the fusion protein Eylea), which carries with it the risk of retinal detachment, hemorrhage, and infection (*7*, *8*). Moreover, their use is limited to advanced disease, and there has been no identifiable end stage to the treatment, with some patients having received in excess of 100 injections in a single eye.

We and others recently reported that the NLRP3 inflammasome is activated in AMD, inducing the production of IL-1β and IL-18, in response to the aggregation of modified host components (*9*–*12*). Our study (*9*) described a role for the NLRP3 inflammasome in protecting against progression to wet AMD, demonstrating that the absence of IL-18—but not IL-1β—signaling resulted in excessive CNV development and suggested that IL-18 specifically regulates angiogenesis in the choroid. We therefore concluded that treatment of late AMD with IL-18 may prevent the onset of CNV (*9*).

Human recombinant IL-18 [GlaxoSmithKline (GSK) clinical asset SB-485232] has already entered a range of clinical trials for the treatment of solid tumors, metastatic melanoma, peritoneal carcinoma, non-Hodgkin's lymphoma, and a range of other cancers (ClinicalTrials.gov identifiers: NCT00107718, NCT00085904, NCT00500058, and NCT00659178) (*13*–*16*). It has been administered intravenously and subcutaneously, and there is now a large cohort of data pertaining to systemic tolerance of recombinant human IL-18 in patients; however, it has never been deployed for use in AMD. Here, we extend our previous findings and

[1]Department of Clinical Medicine, School of Medicine, Trinity College Dublin, Dublin 2, Ireland. [2]National Children's Research Centre, Our Lady's Children's Hospital, Crumlin, Dublin 12, Ireland. [3]Ocular Genetics Unit, Smurfit Institute of Genetics, Trinity College Dublin, Dublin 2, Ireland. [4]School of Biochemistry and Immunology, Immunology Research Centre, Trinity Biomedical Sciences Institute, Trinity College, Dublin 2, Ireland. [5]Research Foundation, Royal Victoria Eye and Ear Hospital, Adelaide Road, Dublin 2, Ireland. [6]National Eye Institute, National Institutes of Health, Bethesda, MD 20892–0001, USA. [7]Trinity Biomedical Sciences Institute, School of Medicine, Trinity College Dublin, Dublin 2, Ireland. [8]Ophthiris Discovery Performance Unit, GlaxoSmithKline, Stevenage SG1 2NY, UK.
*Corresponding author. E-mail: matthew.campbell@tcd.ie (M.C.); sarah.doyle@tcd.ie (S.L.D.)

determine that the use of mature recombinant IL-18 as an antiangiogenic therapy is viable as evidenced by a series of dosing regimes in a murine model of wet AMD. Furthermore, we establish that direct application of recombinant mature IL-18 to the RPE does not induce cell death, as had previously been hypothesized (*10*), and outline a general mechanism for RPE cell death in response to overexpression of the proforms of IL-18 or IL-1β that can be abrogated by autophagy. The use of IL-18 in the treatment of CNV secondary to wet AMD holds immense potential therapeutic value for patients as evidenced by the potency of IL-18 as an antiangiogenic factor in the eye, coupled with its proven safety in human subjects as a systemic agent.

RESULTS

IL-18 is biologically active in primary human and mouse cells

We assessed the activity of the commercially available recombinant mature human IL-18 from R&D Systems alongside the GSK clinical asset, recombinant human IL-18 (SB-485232) (*13*), on natural killer (NK) cells in vitro. Both IL-18 (R&D Systems) and IL-18 (GSK) promoted the degradation of inhibitor of κB (IκB) 5 min after treatment, indicating activation of the nuclear factor κB (NFκB) pathway (Fig. 1A). Both sources of recombinant IL-18 also caused the phosphorylation of p38 mitogen-activated protein kinase (MAPK) after 5 min of treatment, which was maintained over time, demonstrating that IL-18 engaged with its receptor complex to induce the MAPK pathway (Fig. 1A).

IL-18 partly regulates the immune response by inducing interferon-γ (IFN-γ) production in T cells and NK cells. We next assessed the ability of both IL-18 sources to activate NK cells and to promote the induction of IFN-γ. Human peripheral blood mononuclear cells (PBMCs) were left untreated or treated with IL-12, IL-18 (R&D Systems), IL-18 (GSK), or both IL-12 and IL-18 from both sources. IL-18 alone increased the percentage of $CD56^+CD3^-$ NK cells expressing CD69 by about fourfold (Fig. 1B). In conjunction with IL-12, this increased to about 10-fold CD69 induction for both sources of IL-18. Contrary to this, IL-18 alone was not able to induce IFN-γ; however, in conjunction with IL-12, IL-18 strongly promoted IFN-γ induction (Fig. 1C). Similar results were observed when PBMCs were gated for $CD56^+CD3^+$ NK T cells (fig. S1). These data indicate that the clinical asset IL-18 (GSK) acts as expected, paralleling results observed with commercially available IL-18 (R&D Systems).

We repeated flow cytometry analysis using the murine analogs of IL-18 (mIL-18), again sourced from R&D Systems or GSK (named SB-528775) on splenocytes isolated from C57BL/6J mice. Splenocytes were left untreated or treated with IL-12, mIL-18 (R&D Systems), mIL-18 (GSK), or both IL-12 and mIL-18 from both sources. Both sources of mIL-18 up-regulated the expression of CD69 and induced IFN-γ in $NKp46^+NK1.1^+CD3^-$ splenocytes, in conjunction with IL-12; mIL-18 (GSK) was significantly more potent than IL-18 (R&D Systems) (Fig. 1, D and E).

IL-18 is biologically active in RPE cells but does not affect cell viability

Tarallo *et al.* reported that IL-18 was toxic to human RPE cells via an autoregulated and MyD88-dependent pathway (*10*). We next tested whether recombinant human IL-18 (GSK) would cause cell death when administered directly to human RPE cells (ARPE-19 cell line). We measured cell viability in response to increasing doses of IL-18 (GSK). There was no measurable cell death of ARPE-19 cells even at a hyperphysiological dose of 10 μg/ml (Fig. 2A). Furthermore, there were no discernible differences in the morphology of the ARPE-19 cells when treated with increasing doses of IL-18 (GSK) up to and including 10 μg/ml over a 24-hour period (fig. S2A). Furthermore, there was no difference in levels of the tight junction–associated component occludin in these samples, implying that the plasma membrane and tight junction were intact (fig. S2B).

To investigate whether IL-18 could induce cell death in an alternative cell type, we treated human THP1 monocytes with increasing doses of human IL-18 (GSK). Once again, we observed no measurable cell death even at high concentrations of IL-18 (10 μg/ml) (Fig. 2B). In addition, we measured ARPE-19 cell viability at various time points after treatment with IL-18 and observed no significant effects on cell viability (fig. S3).

ARPE-19 cells were also able to respond to IL-18 in a classical sense, as shown by a temporary decrease in IκB in cells treated with IL-18 (Fig. 2C). IκB degradation was also observed in ARPE-19 cells treated with IL-1β, with complete degradation after 10 min and recovery by 60 min (Fig. 2C). We also observed increased phosphorylation of p38 MAPK after stimulation of ARPE-19 cells with either IL-18 or IL-1β (Fig. 2C).

Given the biological activity of IL-18 in mediating IκB degradation, we determined the differential regulation of genes associated with NFκB signaling 6 and 24 hours after stimulation of ARPE-19 cells with human IL-18 (GSK). Of 84 genes, we observed significant differences in only 8 genes at the 6-hour time point and 7 genes at the 24-hour time point (Fig. 2D). No other NFκB-associated genes were differentially regulated at these time points (figs. S4 and S5).

Following our previous findings that IL-18 had antiangiogenic properties in the rodent eye (*9*) with respect to CNV development, we sought to elucidate differential regulation of expression of angiogenesis- and immune-associated components 24 hours after treatment of ARPE-19 cells with IL-18. We observed only decreases in angiogenesis-associated proteins and cytokines, with no up-regulation of any component tested (Fig. 2E and fig. S6).

ARPE-19 cells are a commonly used cell line in ophthalmic research; however, this cell line differs considerably in both phenotype and genotype from native RPE cells (*17*). Hence, we ascertained the effects of IL-18 on primary human RPE cells from three donors (see fig. S7 for donor genotypes). We observed no apoptosis/necrosis or change in morphology after treating the primary RPE cells for 24 hours with increasing doses of IL-18 (fig. S8).

To determine whether there were any adverse effects on plasma membrane and tight junction integrity, we stained monolayers of primary RPE cells for zonula occludens-1 (ZO-1)—a scaffolding protein localized at tight junctions and expressed at the apical periphery of RPE cells. We observed no change in the pattern of ZO-1 staining at the cell peripheries, and punctate ZO-1 staining was observed up to and including stimulation of cells for 24 hours with IL-18 (1 μg/ml) (Fig. 2F). Confocal, three-dimensional Z-stack imaging showed that the apical expression of ZO-1 was unaffected after treatment of cells with IL-18 (fig. S9). ZO-1 levels after treatment with mature IL-18 showed no change with increasing doses of IL-18 (fig. S10).

Pro–IL-18 and pro–IL-1β overexpression causes RPE cell swelling

Our observations that mature recombinant IL-18 was unable to induce RPE cell death despite being biologically active in this cell type did not correlate with the mechanism proposed in (*10*). To investigate this

discrepancy, we looked to the immature precursor of active IL-18, called pro–IL-18. We transfected ARPE-19 cells with vectors expressing pro–IL-18 or pro–IL-1β and analyzed cell morphology 24 hours later (Fig. 3, A and B). ARPE-19 cells overexpressing pro–IL-18 or pro–IL-1β swelled—rather than apoptosed or blebbed—at concentrations of complementary DNA (cDNA) ranging from 10 to 1000 ng/ml (fig. S11). At the highest concentration of pro–IL-18 or pro–IL-1β (1000 ng/ml), cell integrity was completely compromised even in cells transfected with an empty vector (fig. S11, C and D).

Overexpressing pro–IL-18 and pro–IL-1β induced the expression of NLRP3 in ARPE-19 cells, the expression of which was low otherwise (Fig. 3A), suggesting transcriptional induction of NLRP3. To investigate whether NLRP3 inflammasome component expression was causing this RPE cell swelling, we treated ARPE-19 cells for 3 hours with IL-1α or tumor necrosis factor–α (TNF-α) (Fig. 3C) to induce expression of NLRP3, pro–caspase-1, and pro–IL-1β. Cells were then treated with adenosine triphosphate (ATP) to activate the NLRP3 inflammasome. RPE cell swelling was again clearly evident within a short period of time (Fig. 3C). These findings suggest that classical NLRP3 inflammasome activation causes RPE cell swelling.

We next investigated the effects of pro–IL-18 overexpression in vivo in murine RPE. An adeno-associated virus (AAV) vector expressing

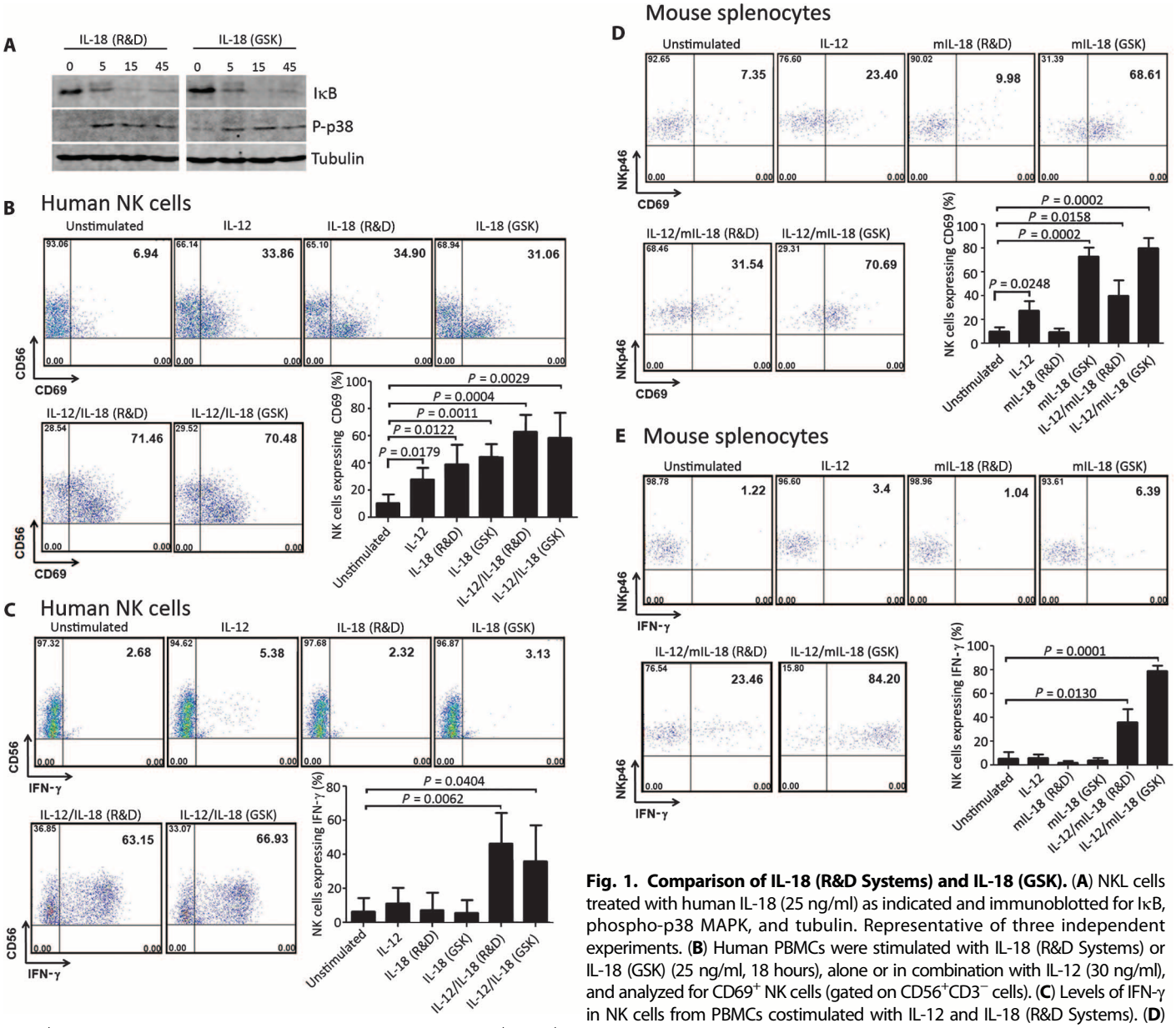

Fig. 1. Comparison of IL-18 (R&D Systems) and IL-18 (GSK). (**A**) NKL cells treated with human IL-18 (25 ng/ml) as indicated and immunoblotted for IκB, phospho-p38 MAPK, and tubulin. Representative of three independent experiments. (**B**) Human PBMCs were stimulated with IL-18 (R&D Systems) or IL-18 (GSK) (25 ng/ml, 18 hours), alone or in combination with IL-12 (30 ng/ml), and analyzed for $CD69^+$ NK cells (gated on $CD56^+CD3^-$ cells). (**C**) Levels of IFN-γ in NK cells from PBMCs costimulated with IL-12 and IL-18 (R&D Systems). (**D**) $CD69^+$ NK cells in C57BL/6J mouse splenocytes (gated on $NKp46^+NK1.1^+CD3^-$ NK cells) stimulated with IL-18 (GSK) (25 ng/ml, 18 hours) with or without IL-12 (10 ng/ml). (**E**) Intracellular IFN-γ in mouse NK cells from splenocytes costimulated with IL-12 and mIL-18 (R&D Systems). Data in (B) and (C) are means ± SEM ($n = 4$ human donors). Data in (D) and (E) are means ± SEM ($n = 5$ mice, three independent experiments). *P* values in (B) to (E) were determined by analysis of variance (ANOVA) with Dunnett's multiple comparison test.

mouse pro–IL-18 cDNA, which could drive the expression of enhanced green fluorescent protein (eGFP), was administered subretinally to wild-type mice. Two weeks after inoculation of this AAV, RPE cell swelling and pro–IL-18 expression were observed within the RPE and neural retina of wild-type mice (Fig. 3E, top panels). *Nlrp3*$^{-/-}$ mice displayed an identical phenotype to the wild-type mice with subretinal administration of pro–IL-18 (Fig. 3E, bottom panels), suggesting that the RPE cell swelling induced by pro–IL-18 was independent of the NLRP3 inflammasome. Quantitative analysis of RPE cell swelling in retinal cryosections showed no significant difference between wild-type and *Nlrp3*$^{-/-}$ mice (Fig. 3F). The pattern and extent of AAV transduction in wild-type and *Nlrp3*$^{-/-}$ retinas are shown in fig. S12.

To assess the impact of pro–IL-18 on the integrity of the neural retina in vivo in real time, we assessed the laminar structure of the neural retina using optical coherence tomography (OCT) in wild-type and *Nlrp3*$^{-/-}$ mice 2 weeks after subretinal injection of the pro–IL-18 AAV. Although the swollen RPE cells were clearly visible by OCT in both wild-type and *Nlrp3*$^{-/-}$ mice (Fig. 3G), there was no significant impact on the integrity of the neural retina, as assessed by examining the thickness of the outer nuclear layer (ONL) (Fig. 3H). This implies that, kinetically, the cell swelling induced by pro–IL-18 is RPE-specific.

After 3 months, rod-isolated electroretinography (ERG) showed a diminished readout when pro–IL-18 was overexpressed in the RPE of wild-type mice (fig. S13A), indicating vision impairment. Histological examination of the retinas of wild-type mice 2 weeks after injection of the pro–IL-18 AAV showed the cell swelling phenotype persisting in the RPE even at AAV titers as low as 0.75×10^{11} genome copies/ml (fig. S13B). Although cell swelling was still evident in some RPE cells, with some RPE cell debris (possibly cell lysis), the ONL had diminished to 2 to 3 rows of nuclei (about 20 μm) (fig. S13C) from about 12 to 14 rows, likely as a result of RPE cell death over time.

Because there was no evidence of apoptosis occurring in ARPE-19 cells after overexpression of pro–IL-18 or pro–IL-1β (Fig. 3B), we ascertained if other cell death mechanisms were evident by analyzing the differential expression of 84 human genes associated with necrosis.

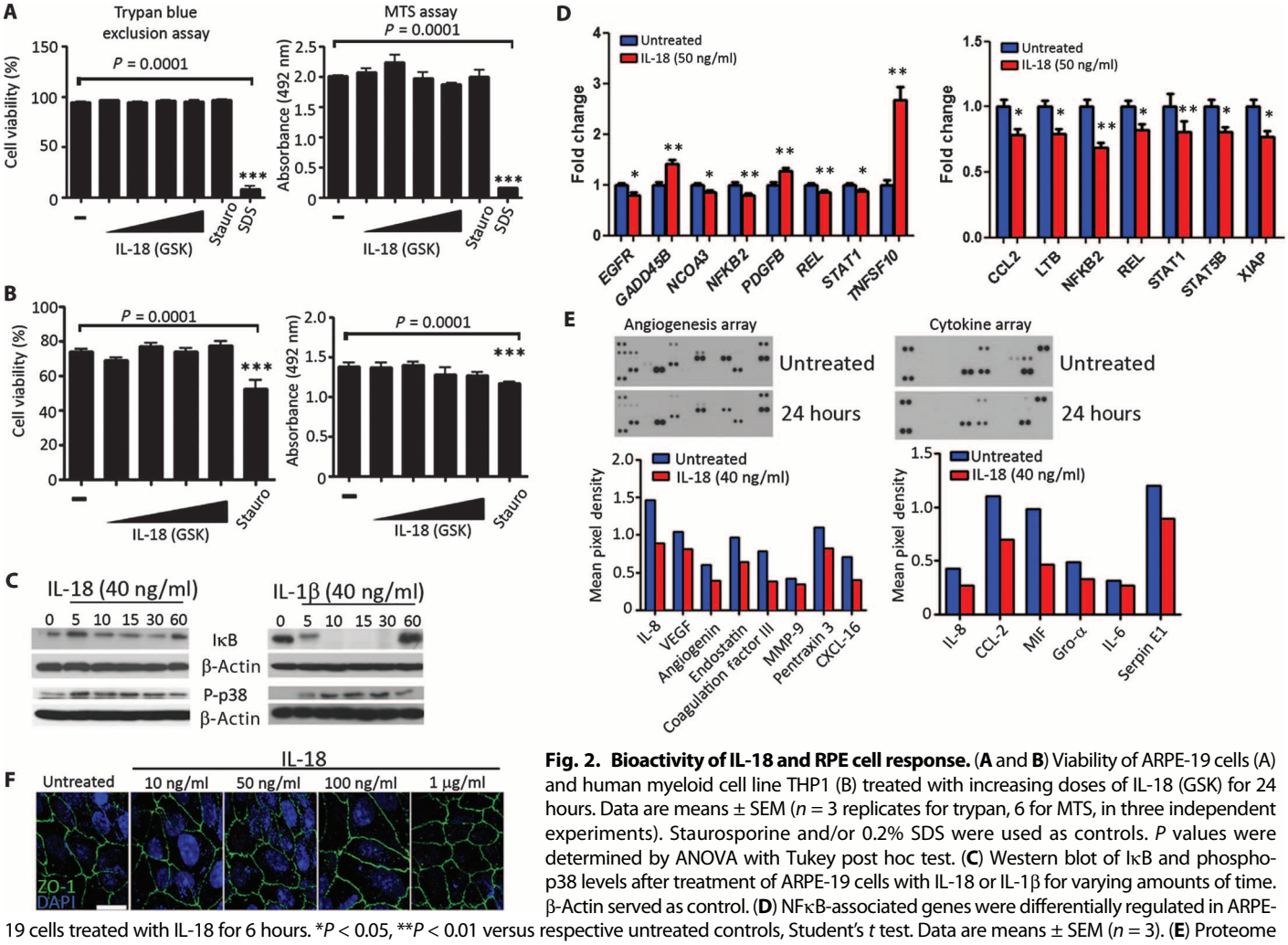

Fig. 2. Bioactivity of IL-18 and RPE cell response. (**A** and **B**) Viability of ARPE-19 cells (A) and human myeloid cell line THP1 (B) treated with increasing doses of IL-18 (GSK) for 24 hours. Data are means ± SEM ($n = 3$ replicates for trypan, 6 for MTS, in three independent experiments). Staurosporine and/or 0.2% SDS were used as controls. *P* values were determined by ANOVA with Tukey post hoc test. (**C**) Western blot of IκB and phospho-p38 levels after treatment of ARPE-19 cells with IL-18 or IL-1β for varying amounts of time. β-Actin served as control. (**D**) NFκB-associated genes were differentially regulated in ARPE-19 cells treated with IL-18 for 6 hours. $^*P < 0.05$, $^{**}P < 0.01$ versus respective untreated controls, Student's *t* test. Data are means ± SEM ($n = 3$). (**E**) Proteome array analysis of angiogenesis-associated proteins and cytokines in the medium of ARPE-19 cells treated with IL-18 (40 ng/ml) (R&D Systems) for 24 hours. (**F**) Expression and localization of ZO-1 in primary human RPE cells treated with increasing doses of IL-18 (R&D Systems) for 24 hours. Images are representative of two biological repeats on different donors. Scale bar, 20 μm.

ARPE-19 cells were transfected with an empty vector, pro–IL-18 cDNA, or pro–IL-1β cDNA, and RNA was isolated 24 hours later. None of these genes were significantly differentially regulated when pro–IL-18 was overexpressed (fig. S14), whereas only four genes were significantly differentially regulated when pro–IL-1β was overexpressed (fig. S15). These data suggest that the cell swelling and any subsequent cell death in response to pro–IL-18 are regulated at posttranscriptional and/or posttranslational levels.

To conclusively show that pro–IL-18 overexpression did not cause the oligomerization of the inflammasome, murine macrophages stably transfected to overexpress NLRP3 and apoptosis-associated Speck-like protein containing a caspase recruitment domain (ASC)–cerulean were left untreated, treated with ATP, or transfected for 24 hours with either empty vector or mouse pro–IL-18. Although ATP caused ASC oligomerization (speck formation) indicative of NLRP3 inflammasome formation, overexpression of pro–IL-18 did not cause inflammasome formation (fig. S16).

RPE cell swelling is inhibited by the promotion of autophagy

Our observations indicate that cell swelling in response to pro–IL-18 is NLRP3 inflammasome–independent. We investigated whether autophagy was involved in regulating cell swelling induced by pro–IL-18. Western blot analysis showed that transfection of human ARPE-19 cells with either pro–IL-1β or pro–IL-18 constructs resulted in an up-regulation of light chain 3 (LC3-I), a protein involved in autophagy, when compared with an empty vector control (fig. S17A). LC3-II, which is found on autophagosome membranes, was also present after treatment. Retinal cryosections from wild-type mice stained positive for LC3 after subretinal inoculation of pro–IL-18 cDNA (fig. S17B). Punctate LC3 was observed in the RPE, in the region positive for pro–IL-18, suggesting that $LC3^{+}$ autophagosomes form in response to pro–IL-18.

Rapamycin—a pharmacological agent that induces autophagy—inhibited ARPE-19 cell swelling induced by pro–IL-18 and pro–IL-1β (fig. S17C), indicating that promoting autophagy results in the inhibition of pro–IL-18– and pro–IL-1β–mediated cell swelling. Conversely, 3-methyladenine (3-MA), an inhibitor of autophagy, effected no significant difference in the numbers of ARPE-19 cell swelling in response to pro–IL-18 or pro–IL-1β (fig. S17C). Both rapamycin and 3-MA slightly reduced the metabolic status of ARPE-19 cells (fig. S17D), but neither affected cell viability (fig. S17E).

Intravitreal injection of IL-18 attenuates CNV

Here, there were contrasts in the cell death response of RPE cells to mature IL-18 and pro–IL-18. Therefore, we assessed the safety/tolerability of recombinant IL-18 when injected intravitreally in mice. In the study by Tarallo *et al.* (*10*), intravitreal injection of mice with an undisclosed dose of IL-18 (from Medical & Biological Laboratories) was reported to cause RPE-specific cell death. We injected increasing doses of mouse IL-18 (GSK) into the vitreous of C57BL/6J mice [animals used in (*10*)] and enucleated the eyes 24 hours later. We observed abundant dead and dying cells at doses of IL-18 (≥1 μg/ml), but no cell death below this threshold (Fig. 4, A and B). Moreover, the dying cells were distributed throughout the retina and were not concentrated solely at the RPE (Fig. 4A).

We also analyzed retinal function of mice receiving intravitreal injection of IL-18. Although there were evident—yet not significant—decreases in ERG responses

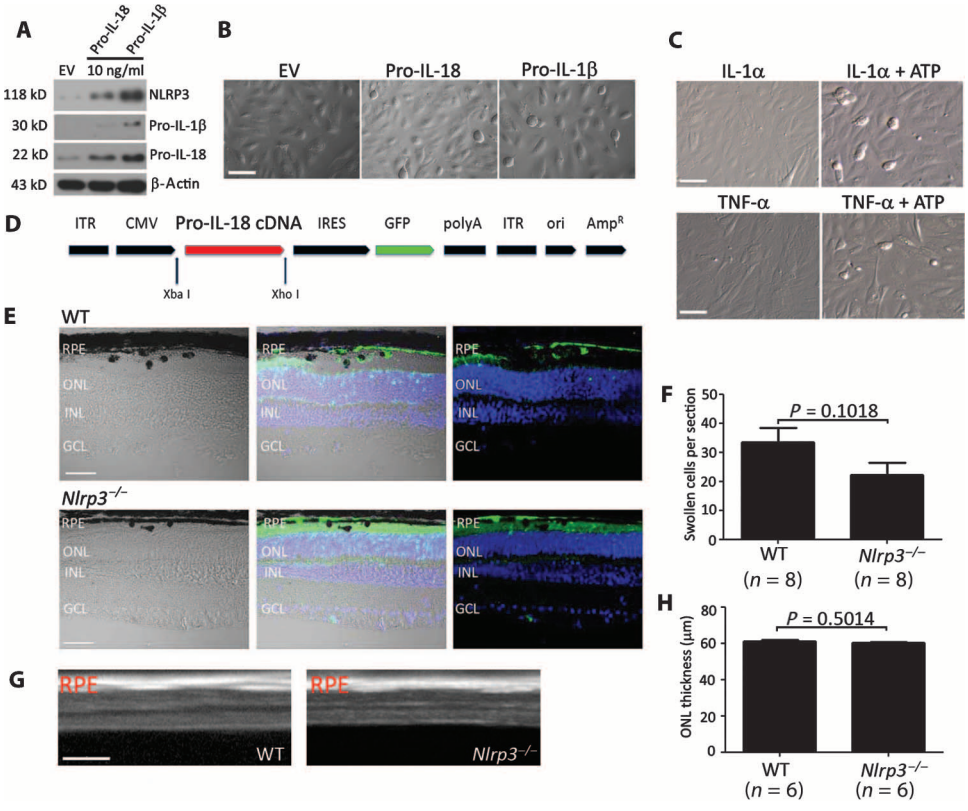

Fig. 3. Cell swelling with overexpression of pro–IL-18 and pro–IL-1β in human RPE cells. (**A** and **B**) Western blot analysis (A) and phase-contrast images (B) of NLRP3, pro–IL-1β, and pro–IL-18 in ARPE-19 cells 24 hours after transfection with empty vector (EV), pro–IL-18 cDNA, or pro–IL-1β cDNA. Treatment with higher concentrations is in fig. S11. Scale bar, 20 μm. (**C**) Phase-contrast images of cells treated with IL-1α or TNF-α (3 hours) ± ATP for 30 min. Scale bars, 20 μm. (**D**) Plasmid map of mouse pro–IL-18 vector driving eGFP expression. ITR, inverted terminal repeat; CMV, cytomegalovirus; IRES, internal ribosome entry site; AmpR, ampicillin resistance. (**E**) Histological sections of wild-type (WT) and *Nlrp3*$^{-/-}$ retinas from eyes injected with pro–IL-18 AAV. OPL, outer plexiform layer; INL, inner nuclear layer; IPL, inner plexiform layer; GCL, ganglion cell layer. Scale bars, 50 μm. (**F**) Number of swollen cells per section of WT and *Nlrp3*$^{-/-}$ mice injected with pro–IL-18–expressing AAV. Data representative of three measurements per retina with eight mice per group. *P* value was determined by Student's *t* test. (**G**) OCT analysis of WT and *Nlrp3*$^{-/-}$ retinas 2 weeks after injection of pro–IL-18 AAV. Scale bar, 200 μm. (**H**) ONL thickness in WT and *Nlrp3*$^{-/-}$ retinas 2 weeks after injection of pro–IL-18 AAV. Data are means of three measurements per retina of ONL thickness ($n = 6$ mice per group). *P* value was determined by Student's *t* test.

after injection of IL-18 (1 μg/ml), these were exceedingly variable (Fig. 4C). Lower doses of IL-18 did not cause any aberrant ERG responses.

Twenty-four hours after injection of IL-18 (200 ng/ml), an immune cell infiltrate was present in the vitreous, but the RPE was perfectly preserved (Fig. 4D). At a nonphysiological dose of IL-18 (1 μg/ml), this immune cell infiltrate was also present with RPE atrophy in some regions. At a physiological dose of 50 ng/ml, IL-18 did not affect the integrity of the retina or the RPE (Fig. 4D). OCT analysis of the retina after intravitreal injection of IL-18 at a range of doses showed numerous vitreal bodies, likely immune cell infiltrates, at a dose of 1 μg/ml, with neural retina enhancements visible in mice injected with IL-18 (200 ng/ml) (Fig. 4E). These features are likely due to activated microvascular endothelial cells and recruitment of systemic immune cells, but this was not investigated.

Given the potent biological activity of IL-18 at doses of 10 to 50 ng/ml, we compared intravitreal administration of IL-18 to anti-VEGF therapy, currently the only available treatment for patients with wet AMD. DMS1529, a murine VEGF-neutralizing domain-specific antibody, which is considered a murine analog of Lucentis and Avastin (used clinically), was injected intravitreally after laser-induced CNV in mice. Similar to a previous report (*18*), DMS1529 decreased CNV volume significantly (Fig. 4F). Injecting DMS1529 in tandem with IL-18 was even more effective at attenuating CNV development than anti-VEGF therapy alone.

Hematopoietic cell–derived IL-18 regulates and prevents laser-induced CNV development

We previously showed that *Il18*$^{-/-}$ mice developed exacerbated CNV (*9*), implying that this cytokine directly regulates CNV development.

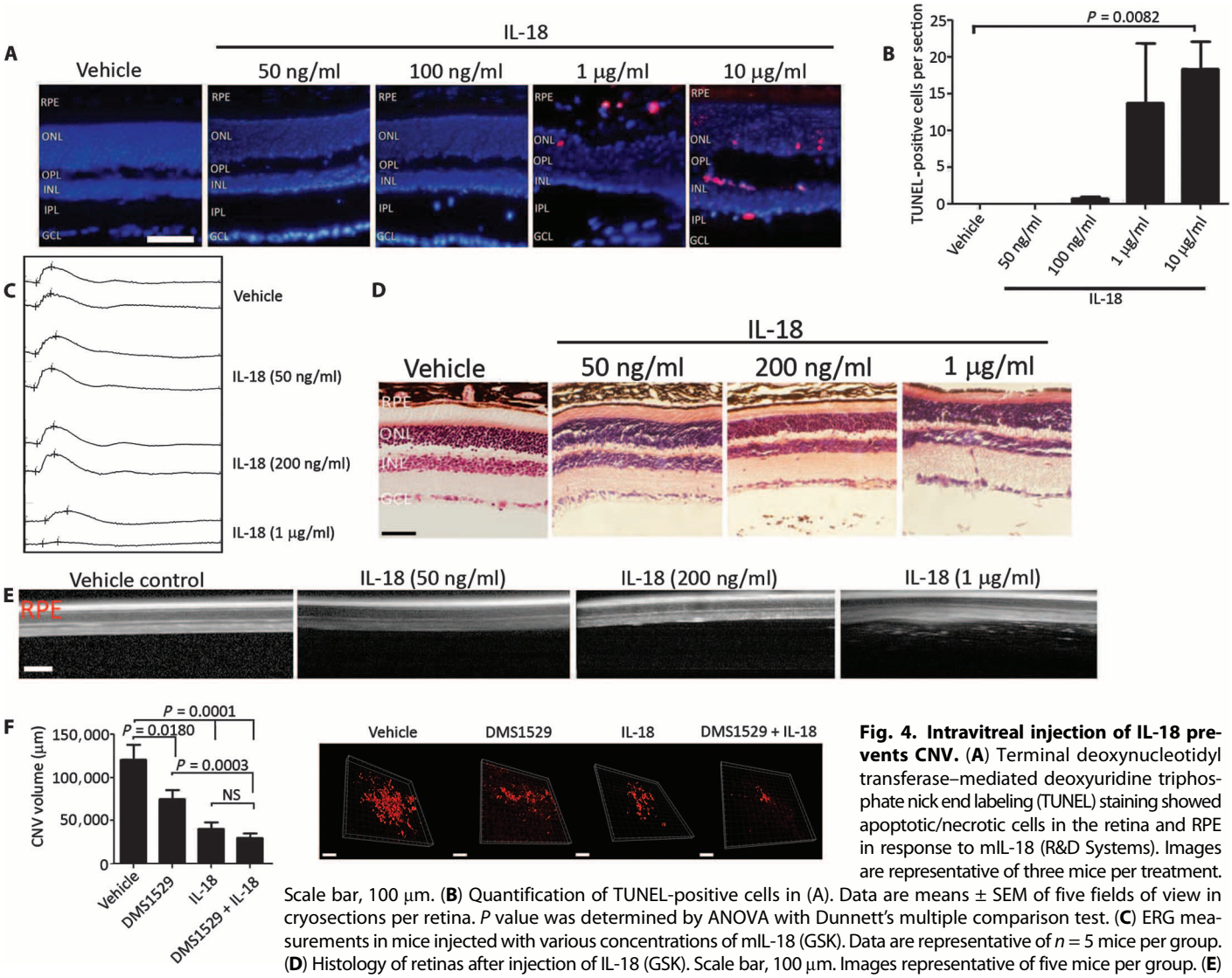

Fig. 4. Intravitreal injection of IL-18 prevents CNV. (**A**) Terminal deoxynucleotidyl transferase–mediated deoxyuridine triphosphate nick end labeling (TUNEL) staining showed apoptotic/necrotic cells in the retina and RPE in response to mIL-18 (R&D Systems). Images are representative of three mice per treatment. Scale bar, 100 μm. (**B**) Quantification of TUNEL-positive cells in (A). Data are means ± SEM of five fields of view in cryosections per retina. *P* value was determined by ANOVA with Dunnett's multiple comparison test. (**C**) ERG measurements in mice injected with various concentrations of mIL-18 (GSK). Data are representative of $n = 5$ mice per group. (**D**) Histology of retinas after injection of IL-18 (GSK). Scale bar, 100 μm. Images representative of five mice per group. (**E**) OCT analysis of retinas injected with mIL-18 (GSK). Scale bar, 200 μm. (**F**) Volume of CNV after intravitreal injection of DMS1529 (10 μg/ml) (mouse anti-VEGF), mIL-18 (50 ng/ml) (GSK), or a combination of the two. Data are means ± SEM ($n = 10$ animals per group). *P* values were determined by ANOVA with Tukey post hoc test. Images to the right are representative of CNV volumes in each experimental group.

To determine whether systemically derived IL-18 could prevent the development of CNV, we generated bone marrow chimeras whereby wild-type mice were irradiated and reconstituted with bone marrow from *Il18*$^{-/-}$ mice and vice versa. Reconstitution was estimated to be 97 to 99% (fig. S15). Similar to *Il18*$^{-/-}$ mice (*9*), *Il18*$^{-/-}$→*Il18*$^{-/-}$ chimeras had significantly greater CNV responses relative to wild-type→wild-type chimeras (Fig. 5A). CNV volume was significantly increased in wild-type mice reconstituted with *Il18*$^{-/-}$ bone marrow, whereas *Il18*$^{-/-}$ mice reconstituted with wild-type bone marrow developed CNV lesions similar to wild-type mice (Fig. 5A). These data indicate that IL-18 derived from hematopoietic cells can protect against CNV development.

We therefore hypothesized that systemic administration of recombinant mature IL-18 could prevent CNV development. At first, we followed the dosing strategy used in previous clinical trials involving systemic IL-18 delivery (*13*–*16*). We administered mIL-18 (GSK) subcutaneously to mice at a dose of 0.1 or 1.0 mg/kg 1 day before and on each day after laser-induced CNV. Both doses of IL-18 significantly attenuated CNV (Fig. 5B), with no observable adverse effects.

Although systemic administration of IL-18 attenuated CNV, the dosing strategy used was based on a clinical trial protocol for use in cancer patients (*13*–*16*). To imitate a realistic dosing strategy for AMD patients, we ascertained whether a single subcutaneous dose of IL-18 could attenuate CNV development. IL-18 (0.1 or 1.0 mg/kg) was administered on the day of laser treatment. Both doses led to a decrease in CNV relative to vehicle control, but these were not significant (Fig. 5C). Administration of IL-18 1 day before laser treatment also had no significant effect on CNV volume (fig. S19); however, IL-18 administered subcutaneously at a dose of 1.0 mg/kg 2 weeks before laser treatment caused a significant reduction in CNV volume (Fig. 5D). Systemically administered IL-18 at a dose of 1.0 mg/kg had no adverse effect on retinal function (Fig. 5E).

Anti-VEGF therapy works more effectively in combination with IL-18

Finally, we analyzed the effect of intravitreal injection of anti-VEGF (DMS1529) in combination with subcutaneous administration of IL-18 (1 mg/kg) (GSK). This combination significantly decreased CNV volume compared to vehicle (Fig. 6A) and was significantly more potent than intravitreal injection of DMS1529 alone (comparing with vehicle control data in Fig. 4F). (Note that this experiment was performed within the same experimental cohort using the same vehicle control at the same time, but data are shown on two different graphs.) Given the translational potential for the use of systemic IL-18 in the treatment of wet AMD, we examined the effect of administering IL-18 (0.1 or 1.0 mg/kg) subcutaneously on the day of CNV and for 3 subsequent days after to reflect a clinical scenario. After 7 days, we noted decreased CNV volume of mIL-18 at both 0.1 and 1 mg/kg (Fig. 6B) and decreased CNV-induced permeability (Fig. 6C).

DISCUSSION

Our previous findings indicated that IL-18 warranted further investigation for its role in regulating CNV development. Although we had demonstrated a protective role for IL-18 in the development of wet AMD

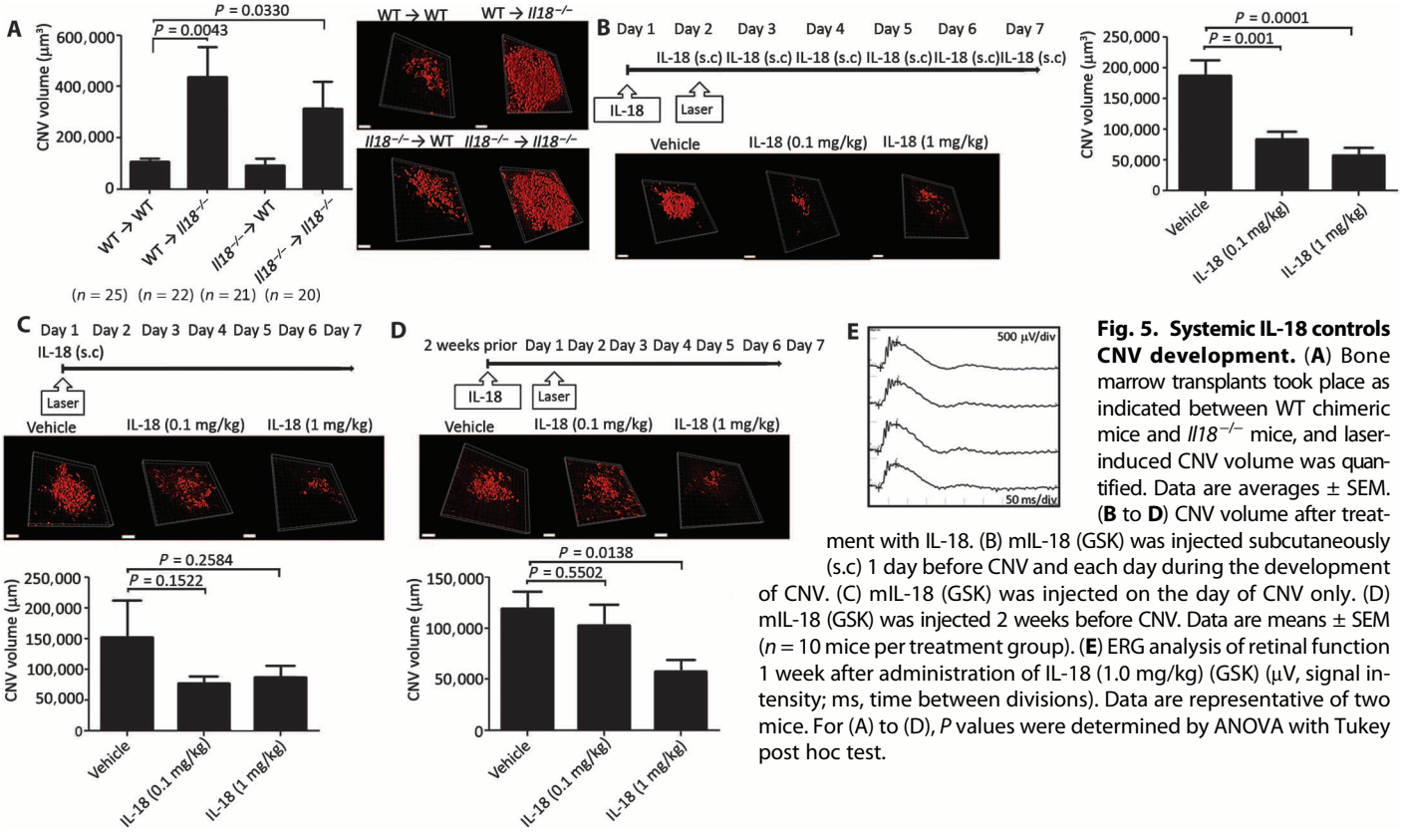

Fig. 5. Systemic IL-18 controls CNV development. (**A**) Bone marrow transplants took place as indicated between WT chimeric mice and *Il18*$^{-/-}$ mice, and laser-induced CNV volume was quantified. Data are averages ± SEM. (**B** to **D**) CNV volume after treatment with IL-18. (B) mIL-18 (GSK) was injected subcutaneously (s.c) 1 day before CNV and each day during the development of CNV. (C) mIL-18 (GSK) was injected on the day of CNV only. (D) mIL-18 (GSK) was injected 2 weeks before CNV. Data are means ± SEM (n = 10 mice per treatment group). (**E**) ERG analysis of retinal function 1 week after administration of IL-18 (1.0 mg/kg) (GSK) (μV, signal intensity; ms, time between divisions). Data are representative of two mice. For (A) to (D), P values were determined by ANOVA with Tukey post hoc test.

(*9*), others had reported that IL-18 played a pathogenic role in the development of geographic atrophy (*10*). We had observed NLRP3 activation in RPE cells in a model of dry AMD (*9*) but had not determined whether it was pathogenic or protective; therefore, we were keen to assess the effect of IL-18 on the RPE. In contrast to Tarallo *et al.* (*10*), we did not observe any change in RPE cell viability or morphology when cells were treated with physiological doses of IL-18. We conclude that although RPE cells are biologically responsive to IL-18, it does not cause cell death when administered exogenously in its mature form. We suggest that the destruction of the RPE reported in (*10*) upon intravitreal administration of IL-18 is due to a response driven by hyperphysiological dosing of IL-18, which draws in an excessive immune cell infiltrate, resulting in nonspecific severe local tissue damage to the retina as a whole.

We initially hypothesized that assembly of the NLRP3 inflammasome itself may cause cell death in RPE cells. Each individual RPE cell is in direct contact with about 25 photoreceptor cells (*19*). This implies that RPE cells would be highly resistant to changes in cell shape given their evolved tight junctions, which comprise the outer blood-retina barrier. Cellular swelling has come to the fore as a key initiator of the NLRP3 inflammasome (*20*). We observed RPE cell swelling simply upon overexpression of either pro–IL-18 or pro–IL-1β. This implied that assembly of the NLRP3 inflammasome in RPE cells may associate with deregulated cell swelling, likely resulting in RPE atrophy. This correlates with observations reported in (*12*), where activation of the NLRP3 inflammasome in ARPE-19 cells resulted in pyroptosis, a process of cell death where cells swell before undergoing lysis. However, upon further investigation, we determined that the cell swelling phenotype observed was NLRP3-independent, because the RPE cells were similarly swollen and distorted in mice lacking NLRP3 as in wild-type mice, after subretinal injection with a pro–IL-18–expressing AAV.

Autophagy is a homeostatic cellular process involved in protein and organelle degradation via the lysosomal pathway, and has been recently linked with the pathogenesis of AMD (*20*–*24*). Autophagy has been shown to control IL-1β secretion by targeting pro–IL-1β for degradation in macrophages (*25*). We investigated whether overexpression of pro–IL-18 might also promote autophagy and whether this could regulate cell swelling. Indeed, autophagy was visible in ARPE-19 cells overexpressing pro–IL-18. Furthermore, when autophagy was promoted, the cell swelling phenotype was inhibited, indicating that autophagy can regulate pathological RPE cell volume, likely owing to sequestration and degradation of the abundant pro–IL-18.

Mature IL-18 was nontoxic to RPE cells. Therefore, we pursued this molecule in this study and have illustrated the potential of recombinant IL-18 as a therapeutic for the treatment of CNV associated with exudative AMD (Fig. 7). IL-18 could be used as an adjunct therapy alongside current antibody-based strategies. However, this cytokine can also work as potently alone as anti-VEGF drugs in these animal models. Current use of Lucentis for the treatment of wet AMD is restricted to intravitreal injection because systemic administration of these antibodies holds considerable risks to subjects owing to other essential homeostatic roles of VEGF (*26*). Our data suggest that IL-18 can be administered systemically.

IL-18 appears to prevent angiogenesis by two methods. First, it acts directly on epithelial and endothelial cells (*9*) as an antiangiogenic factor and antipermeability factor, decreasing VEGF levels as evidenced by the significant restriction on CNV volume when IL-18 is administered on the same day as the laser-induced injury in tandem with anti-VEGF treatment. Second, IL-18 regulation of CNV volume

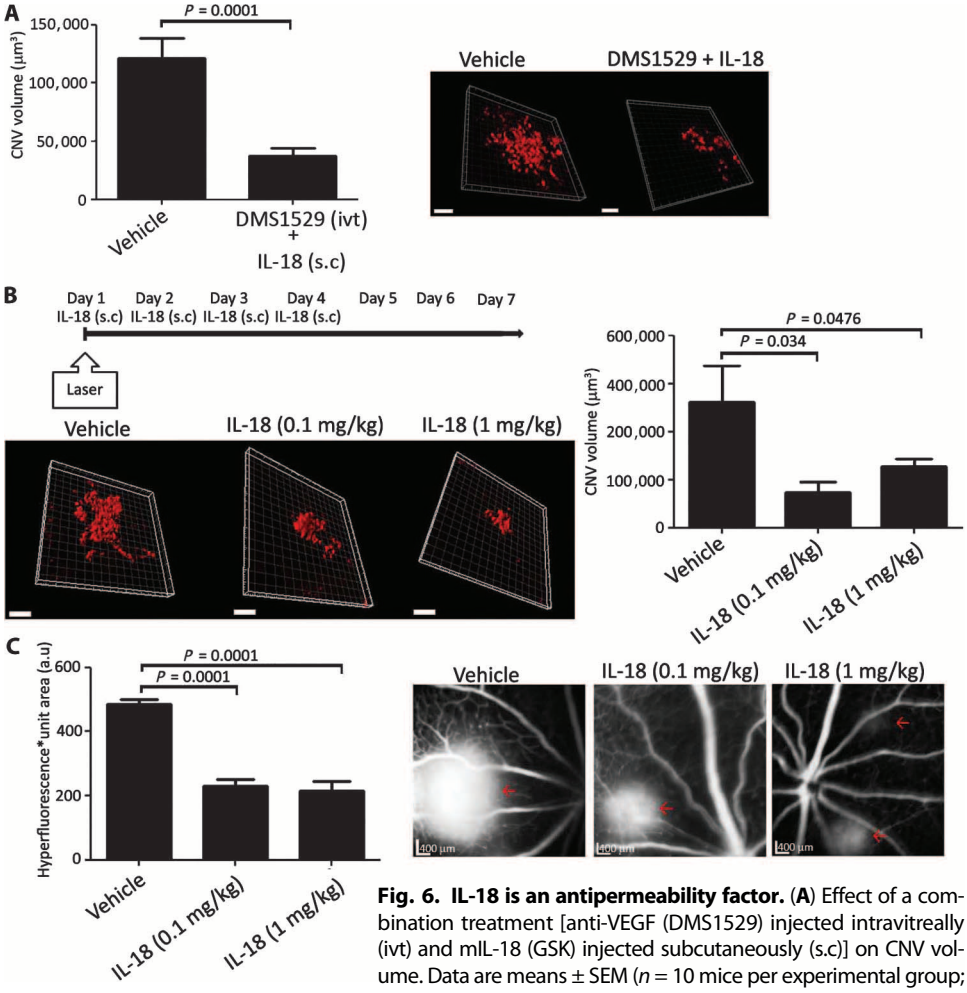

Fig. 6. IL-18 is an antipermeability factor. (**A**) Effect of a combination treatment [anti-VEGF (DMS1529) injected intravitreally (ivt) and mIL-18 (GSK) injected subcutaneously (s.c)] on CNV volume. Data are means ± SEM (n = 10 mice per experimental group; 24 CNV lesions for control and 35 for DMS1529 + IL-18). P value was determined by Student's t test. (**B**) mIL-18 (GSK) was injected on the day of CNV and for 3 days after CNV, and CNV volume was quantified. Data are means ± SEM (n = 11 to 18 CNV lesions, with six mice per experimental group). P values were determined by ANOVA with Tukey post hoc test. (**C**) Vascular permeability in the CNV area upon treatment with mIL-18 (GSK) or vehicle. Data are means ± SEM (n = 8 to 11 CNV lesions). Fluorescein angiography representative of six mice per experimental group. P values were determined by ANOVA with Tukey post hoc test.

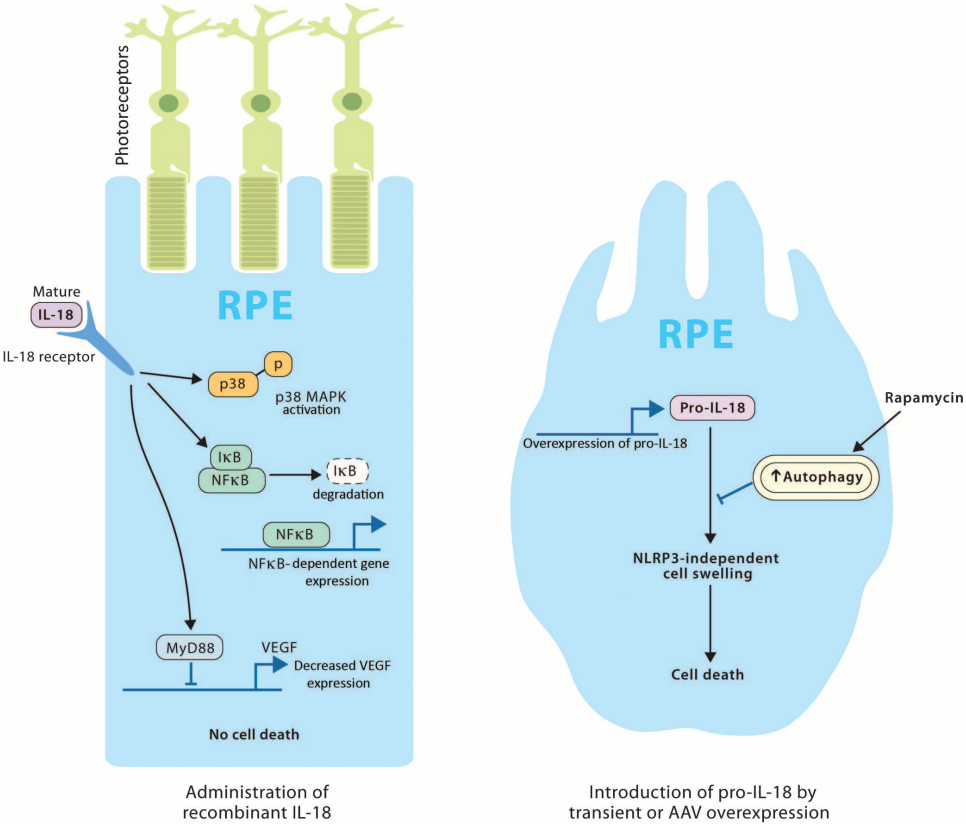

Fig. 7. Schematic representation of pro–IL-18 and mature IL-18 bioactivity in RPE cells. The RPE cell to the left represents the cell response to mature recombinant IL-18. The swollen cell to the right represents the mechanistic response of the RPE cell to overexpression/up-regulation of pro–IL-18.

when administered 2 weeks before laser-induced injury indicates that a subpopulation of cells, as yet uncharacterized, with the capability to restrict angiogenesis are likely being induced by IL-18. Pertinently, its ability to prevent excessive CNV permeability has strong translational potential because this is a hallmark diagnostic feature of CNV development. Although laser-induced CNV does not recapitulate all stages of development of CNV secondary to wet AMD in human subjects, the pathogenesis of lesion development after laser-induced injury appears to be conserved among rodents and primates (*27*) and shares several features with human neovascular AMD. The readouts from this model have been largely predictive of efficacy observed in nonhuman primates and subsequently in human clinical trials (*27*).

Here, we show that IL-18 can be used effectively as a systemic agent. Data already exist showing safety/tolerability of systemic administration of human IL-18 (GSK, SB-485232) in human subjects at doses as high as 2000 μg/kg (*16*). Moreover, ocular abnormalities have not been reported in any clinical study using SB-485232 to date, with no reports of any subject developing symptoms or characteristics of dry AMD (*13*–*16*). IL-18 is a potently proinflammatory cytokine; for this reason, attempting to actively increase its systemic levels as a form of therapy might raise concerns regarding the risk of sending the immune system into overdrive. Dosing of patients with SB-485232 induces low levels of IFN-γ and may result in grade 1 to 2 transient fevers (*15*), which are manageable and rapidly resolve. These characteristics of IL-18 biology are of substantial comfort when considering the use of recombinant IL-18 as a therapy for preventing CNV in end-stage AMD. Our findings represent a potential new therapeutic strategy for the treatment of this incurable disease.

MATERIALS AND METHODS

Study design

Given previous descriptions on the role of IL-18 in regulating ocular angiogenesis, we sought to determine the therapeutic benefit of mature recombinant IL-18. In addition, we assessed the safety of mature IL-18 on human RPE cells because it has been reported in the literature that IL-18 specifically caused RPE cell apoptosis. We used both RPE cell lines and primary RPE cells to define issues surrounding IL-18–mediated toxicity, and we used the laser-induced model of CNV to determine the effect of IL-18 in regulating CNV development. This model has proven effective at predicting efficacious therapies for the treatment of AMD (*27*). Littermate controls were used in all animal experiments, and 10 mice were used per experimental group to allow for robust statistical analysis to be made of each CNV formed. During assessment of CNV volumes using Z-stack confocal imaging, the individual collecting data had access only to cage allocation of mice and was blinded to treatment. The same conditions applied when determining volumes quantitatively.

Cell culture

Human ARPE-19 cells (American Type Culture Collection CRL 2302, LGC Promochem), THP1 cells (European Collection of Cell Cultures), and NKL cell line [C. Gardiner, Trinity College Dublin (TCD)] were used. Primary PBMCs were isolated from human blood. Cells were cultured at 37°C, 5% CO_2, 95% air in a 1:1 mixture of Dulbecco's modified Eagle's medium and Ham's F12 medium with sodium bicarbonate (1.2 g/liter), 2.5 mM L-glutamine, 15 mM Hepes, and 0.5 mM sodium pyruvate (Sigma-Aldrich) with 10% fetal calf serum. Immortalized macrophages stably transfected with a construct for the overexpression of cerulean-tagged mouse ASC in tandem with NLRP3-FLAG were used essentially as described previously (*28*).

Transfection of human pro–IL-18 and human pro–IL-1β

Human pro–IL-18 cDNA in a pCMV6-XL5–based vector or human pro–IL-1β cDNA was transfected into ARPE-19 cells with Lipofectamine 2000 (Invitrogen) according to the manufacturer's instructions.

Murine models of CNV

All animal studies were ethically reviewed and carried out in accordance with Animals (Scientific Procedures) Act 1986 and the GSK Policy on the Care, Welfare and Treatment of Animals. All relevant national and

institutional approvals were obtained before commencement of the work. CNV was induced in wild-type C57BL/6J mice ($n = 10$ mice per experimental group) with a green 532-nm Iridex Iris laser (532 nm, 140 mW, 100 ms, 50-μm spot size, three spots per eye) incorporating a microscopic delivery system as described previously (*9*). After laser burn, DMS1529 (GSK) or mIL-18 (GSK SB-528775) was injected intravitreally or subcutaneously. Mice were sacrificed 6 days after experiment, and neural retina was removed. Eye cups were incubated with a Griffonia–simplicifolia–isolectin–Alexa 568 (Molecular Probes) (1:300 in phosphate-buffered saline) overnight at 4°C, and CNV was assessed by confocal microscopy.

Bone marrow chimera generation

Lethally irradiated CD45.1$^+$ (PepBoy) or CD45.2$^+$ C57BL/6J and *Il18*$^{-/-}$ recipient mice (9 Gy in two doses, 3 hours apart) were each reconstituted with 1×10^7 bone marrow cells from donor CD45.2$^+$ C57BL/6J mice or *Il18*$^{-/-}$ mice, isolated from the tibias and femurs. To ensure efficient irradiation and reconstitution, expression of CD45.1 versus CD45.2 was assessed in the blood after 4 weeks by fluorescence-activated cell sorting (FACS) analysis (fig. S18). CNV was induced in mice 6 weeks after irradiation.

Statistical analyses

Statistical analysis was performed with Student's *t* test, with significance represented by a *P* value of ≤0.05 when two individual experimental groups were analyzed. For multiple comparisons, as was the case in the multiple comparisons of CNV volume in Figs. 4 to 6, ANOVA was used with a Tukey-Kramer post-test and significance was represented by a *P* value of ≤0.05. Each laser-induced lesion was used as an independent observation in the CNV volume analysis, and 10 mice were used in each experimental group. Two-tailed tests were used throughout, and the statistical approaches were all deemed to be valid for each individual experiment, that is, the data were normally distributed.

SUPPLEMENTARY MATERIALS

www.sciencetranslationalmedicine.org/cgi/content/full/6/230/230ra44/DC1
Materials and Methods
Fig. S1. Analysis of human NK cells.
Fig. S2. Effect of IL-18 on RPE cell integrity.
Fig. S3. Viability of RPE cells after IL-18 treatment.
Fig. S4. Differentially regulated NFκB-associated genes 6 hours after IL-18 treatment.
Fig. S5. Differentially regulated NFκB-associated genes 24 hours after IL-18 treatment.
Fig. S6. Decrease in angiogenesis-associated proteins and cytokines after IL-18 treatment.
Fig. S7. Primary RPE cell characterization.
Fig. S8. No apoptosis or necrosis of RPE cells after treatment with IL-18.
Fig. S9. ZO-1 expression in RPE cells.
Fig. S10. Western blot and densitometric quantification of ZO-1 in primary RPE cells.
Fig. S11. Human RPE cell response to pro–IL-18 and pro–IL-1β.
Fig. S12. Cell swelling after expression of pro–IL-18.
Fig. S13. Pro–IL-18 expression in RPE for 3 months.
Fig. S14. Necrosis gene array after transfection of RPE cells with pro–IL-18.
Fig. S15. Necrosis gene array after transfection of RPE cells with pro–IL-1β.
Fig. S16. Mouse ASC-cerulean oligomerization.
Fig. S17. Autophagy prevents RPE cell swelling induced by pro–IL-18 expression.
Fig. S18. Bone marrow chimera reconstitution.
Fig. S19. IL-18 injected 1 day before CNV has no effect on lesion volume.

REFERENCES AND NOTES

1. D. B. Rein, J. S. Wittenborn, X. Zhang, A. A. Honeycutt, S. B. Lesesne, J. Saaddine; Vision Health Cost-Effectiveness Study Group, Forecasting age-related macular degeneration through the year 2050: The potential impact of new treatments. *Arch. Ophthalmol.* **127**, 533–540 (2009).
2. C. A. Janeway, R. Medzhitov, Innate immune recognition. *Annu. Rev. Immunol.* **20**, 197–216 (2002).
3. L. A. O'Neill, A. G. Bowie, The family of five: TIR-domain-containing adaptors in Toll-like receptor signalling. *Nat. Rev. Immunol.* **7**, 353–364 (2007).
4. K. Schroder, J. Tschopp, The inflammasomes. *Cell* **140**, 821–832 (2010).
5. R. D. Jager, W. F. Mieler, J. W. Miller, Age-related macular degeneration. *N. Engl. J. Med.* **358**, 2606–2617 (2008).
6. CATT Research Group; D. F. Martin, M. G. Maguire, G. S. Ying, J. E. Grunwald, S. L. Fine, G. J. Jaffe, Ranibizumab and bevacizumab for neovascular age-related macular degeneration. *N. Engl. J. Med.* **364**, 1897–1908 (2011).
7. J. S. Heier, D. M. Brown, V. Chong, J. F. Korobelnik, P. K. Kaiser, Q. D. Nguyen, B. Kirchhof, A. Ho, Y. Ogura, G. D. Yancopoulos, N. Stahl, R. Vitti, A. J. Berliner, Y. Soo, M. Anderesi, G. Groetzbach, B. Sommerauer, R. Sandbrink, C. Simader, U. Schmidt-Erfurth; VIEW 1 and VIEW 2 Study Groups, Intravitreal aflibercept (VEGF Trap-Eye) in wet age-related macular degeneration. *Ophthalmology* **119**, 2537–2548 (2012).
8. K. Kinnunen, G. Petrovski, M. C. Moe, A. Berta, K. Kaarniranta, Molecular mechanisms of retinal pigment epithelium damage and development of age-related macular degeneration. *Acta Ophthalmol.* **90**, 299–309 (2012).
9. S. L. Doyle, M. Campbell, E. Ozaki, R. G. Salomon, A. Mori, P. F. Kenna, G. J. Farrar, A. S. Kiang, M. M. Humphries, E. C. Lavelle, L. A. O'Neill, J. G. Hollyfield, P. Humphries, NLRP3 has a protective role in age-related macular degeneration through the induction of IL-18 by drusen components. *Nat. Med.* **18**, 791–798 (2012).
10. V. Tarallo, Y. Hirano, B. D. Gelfand, S. Dridi, N. Kerur, Y. Kim, W. G. Cho, H. Kaneko, B. J. Fowler, S. Bogdanovich, R. J. Albuquerque, W. W. Hauswirth, V. A. Chiodo, J. F. Kugel, J. A. Goodrich, S. L. Ponicsan, G. Chaudhuri, M. P. Murphy, J. L. Dunaief, B. K. Ambati, Y. Ogura, J. W. Yoo, D. K. Lee, P. Provost, D. R. Hinton, G. Núñez, J. Z. Baffi, M. E. Kleinman, J. Ambati, DICER1 loss and *Alu* RNA induce age-related macular degeneration via the NLRP3 inflammasome and MyD88. *Cell* **149**, 847–859 (2012).
11. A. Kauppinen, H. Niskanen, T. Suuronen, K. Kinnunen, A. Salminen, K. Kaarniranta, Oxidative stress activates NLRP3 inflammasomes in ARPE-19 cells—Implications for age-related macular degeneration (AMD). *Immunol. Lett.* **147**, 29–33 (2012).
12. W. A. Tseng, T. Thein, K. Kinnunen, K. Lashkari, M. S. Gregory, P. A. D'Amore, B. R. Ksander, NLRP3 inflammasome activation in retinal pigment epithelial cells by lysosomal destabilization: Implications for age-related macular degeneration. *Invest. Ophthalmol. Vis. Sci.* **54**, 110–120 (2013).
13. A. A. Tarhini, M. Millward, P. Mainwaring, R. Kefford, T. Logan, A. Pavlick, S. J. Kathman, K. H. Laubscher, M. M. Dar, J. M. Kirkwood, A phase 2, randomized study of SB-485232, rhIL-18, in patients with previously untreated metastatic melanoma. *Cancer* **115**, 859–868 (2009).
14. M. J. Robertson, J. M. Kirkwood, T. F. Logan, K. M. Koch, S. Kathman, L. C. Kirby, W. N. Bell, L. M. Thurmond, J. Weisenbach, M. M. Dar, A dose-escalation study of recombinant human interleukin-18 using two different schedules of administration in patients with cancer. *Clin. Cancer Res.* **14**, 3462–3469 (2008).
15. M. J. Robertson, J. W. Mier, T. Logan, M. Atkins, H. Koon, K. M. Koch, S. Kathman, L. N. Pandite, C. Oei, L. C. Kirby, R. C. Jewell, W. N. Bell, L. M. Thurmond, J. Weisenbach, S. Roberts, M. M. Dar, Clinical and biological effects of recombinant human interleukin-18 administered by intravenous infusion to patients with advanced cancer. *Clin. Cancer Res.* **12**, 4265–4273 (2006).
16. J. Golab, T. Stoklosa, Technology evaluation: SB-485232, GlaxoSmithKline. *Curr. Opin. Mol. Ther.* **7**, 85–93 (2005).
17. N. V. Strunnikova, A. Maminishkis, J. J. Barb, F. Wang, C. Zhi, Y. Sergeev, W. Chen, A. O. Edwards, D. Stambolian, G. Abecasis, A. Swaroop, P. J. Munson, S. S. Miller, Transcriptome analysis and molecular signature of human retinal pigment epithelium. *Hum. Mol. Genet.* **19**, 2468–2486 (2010).
18. S. J. Robbie, P. Lundh von Leithner, M. Ju, C. A. Lange, A. G. King, P. Adamson, D. Lee, C. Sychterz, P. Coffey, Y. S. Ng, J. W. Bainbridge, D. T. Shima, Assessing a novel depot delivery strategy for noninvasive administration of VEGF/PDGF RTK inhibitors for ocular neovascular disease. *Invest. Ophthalmol. Vis. Sci.* **54**, 1490–1500 (2013).
19. J. R. Sparrow, M. Boulton, RPE lipofuscin and its role in retinal pathobiology. *Exp. Eye Res.* **80**, 595–606 (2005).
20. V. Compan, A. Baroja-Mazo, G. López-Castejón, A. I. Gomez, C. M. Martínez, D. Angosto, M. T. Montero, A. S. Herranz, E. Bazán, D. Reimers, V. Mulero, P. Pelegrín, Cell volume regulation modulates NLRP3 inflammasome activation. *Immunity* **37**, 487–500 (2012).
21. J. Viiri, M. Amadio, N. Marchesi, J. M. Hyttinen, N. Kivinen, R. Sironen, K. Rilla, S. Akhtar, A. Provenzani, V. G. D'Agostino, S. Govoni, A. Pascale, H. Agostini, G. Petrovski, A. Salminen, K. Kaarniranta, Autophagy activation clears ELAVL1/HuR-mediated accumulation of SQSTM1/p62 during proteasomal inhibition in human retinal pigment epithelial cells. *PLOS One* **8**, 1–16 (2013).
22. K. Kaarniranta, D. Sinha, J. Blasiak, A. Kauppinen, Z. Veréb, A. Salminen, M. E. Boulton, G. Petrovski, Autophagy and heterophagy dysregulation leads to retinal pigment epithelium dysfunction and development of age-related macular degeneration. *Autophagy* **9**, 973–984 (2013).
23. A. L. Wang, T. J. Lukas, M. Yuan, N. Du, M. O. Tso, A. H. Neufeld, Autophagy and exosomes in the aged retinal pigment epithelium: Possible relevance to drusen formation and age-related macular degeneration. *PLOS One* **4**, e4160 (2009).

24. T. U. Krohne, N. K. Stratmann, J. Kopitz, F. G. Holz, Effects of lipid peroxidation products on lipofuscinogenesis and autophagy in human retinal pigment epithelial cells. *Exp. Eye Res.* **90**, 465–471 (2010).
25. J. Harris, M. Hartman, C. Roche, S. G. Zeng, A. O'Shea, F. A. Sharp, E. M. Lambe, E. M. Creagh, D. T. Golenbock, J. Tschopp, H. Kornfeld, K. A. Fitzgerald, E. C. Lavelle, Autophagy controls IL-1β secretion by targeting pro-IL-1β for degradation. *J. Biol. Chem.* **286**, 9587–9597 (2011).
26. A. A. Moshfeghi, P. J. Rosenfeld, C. A. Puliafito, S. Michels, E. N. Marcus, J. D. Lenchus, A. S. Venkatraman, Systemic bevacizumab (Avastin) therapy for neovascular age-related macular degeneration: Twenty-four-week results of an uncontrolled open-label clinical study. *Ophthalmology* **113**, 2002.e1–2002.e12 (2006).
27. H. E. Grossniklaus, S. J. Kang, L. Berglin, Animal models of choroidal and retinal neovascularization. *Prog. Retin. Eye Res.* **29**, 500–519 (2010).
28. F. G. Bauernfeind, G. Horvath, A. Stutz, E. S. Alnemri, K. MacDonald, D. Speert, T. Fernandes-Alnemri, J. Wu, B. G. Monks, K. A. Fitzgerald, V. Hornung, E. Latz, Cutting edge: NF-κB activating pattern recognition and cytokine receptors license NLRP3 inflammasome activation by regulating NLRP3 expression. *J. Immunol.* **183**, 787–791 (2009).

Acknowledgments: We thank C. Woods, C. Murray, and D. Flynn for animal husbandry. We also thank the Research Foundation at the Royal Victoria Eye and Ear Hospital for assistance in the acquisition of the Iridex laser system. **Funding:** Enterprise Ireland, GSK, Science Foundation Ireland (SFI) (12/YI/B2614), and BrightFocus Foundation. The Ocular Genetics Unit at TCD is supported by SFI, the Health Research Board of Ireland, Irish Research Council for Science Engineering and Technology, the United States Department of Defense (Telemedicine and Advanced Technology Research Center), and the European Research Council. **Author contributions:** S.L.D. conceived, designed, and performed the experiments and wrote the paper. E.O. performed the experiments. K.B. performed FACS and Western blot analyses. M.M.H. generated AAVs and genotyped cells. K.M. and J.K. performed Western blot analysis. P.F.K. performed ERG analyses. A.M. isolated primary human RPE cells. A.-S.K. analyzed the data. S.P.S. and E.H. established bone marrow chimeras. E.C.L. designed and analyzed autophagy-related experiments. C.G. designed IL-18 bioactivity assays. P.G.F. designed bone marrow chimera experiments. P.A. designed and directed experiments surrounding therapeutic use of IL-18. P.H. contributed to design and analysis of experiments. M.C. conceived, designed, and performed the experiments and wrote the paper. **Competing interests:** TCD owns intellectual property surrounding the use of IL-18 for wet AMD treatment. GSK owns intellectual property surrounding the use of IL-18 for a range of cancers. **Data and materials availability:** SB-485232 and SB-528775 were used under a material transfer agreement (MTA) between TCD and GSK. Primary human RPE cells were used under an MTA between TCD and the U.S. NIH.

Submitted 17 September 2013
Accepted 13 February 2014
Published 2 April 2014
10.1126/scitranslmed.3007616

Citation: S. L. Doyle, E. Ozaki, K. Brennan, M. M. Humphries, K. Mulfaul, J. Keaney, P. F. Kenna, A. Maminishkis, A.-S. Kiang, S. P. Saunders, E. Hams, E. C. Lavelle, C. Gardiner, P. G. Fallon, P. Adamson, P. Humphries, M. Campbell, IL-18 attenuates experimental choroidal neovascularization as a potential therapy for wet age-related macular degeneration. *Sci. Transl. Med.* **6**, 230ra44 (2014).

Science Translational Medicine
AAAS

IL-18 Attenuates Experimental Choroidal Neovascularization as a Potential Therapy for Wet Age-Related Macular Degeneration

Sarah L. Doyle, Ema Ozaki, Kiva Brennan, Marian M. Humphries, Kelly Mulfaul, James Keaney, Paul F. Kenna, Arvydas Maminishkis, Anna-Sophia Kiang, Sean P. Saunders, Emily Hams, Ed C. Lavelle, Clair Gardiner, Padraic G. Fallon, Peter Adamson, Peter Humphries and Matthew Campbell (April 2, 2014)

Science Translational Medicine **6** (230), 230ra44. [doi: 10.1126/scitranslmed.3007616]

Editor's Summary

Treating Age-Related Macular Degeneration with IL-18

Age-related macular degeneration (AMD) comes in two forms: "wet" and "dry." Dry AMD is characterized by the death of various eye cells, whereas wet AMD arises from the formation of new blood vessels in the choroid. The only treatment for AMD is antibodies against growth factors that regulate vascular growth; this is not a cure, but rather a chronic therapy requiring direct injection into the eye. Seeking out a new therapy, Doyle and colleagues found that an inflammatory cytokine, interleukin-18 (IL-18), works to prevent neovascularization in animal models. The eyes of mice were hit with a laser to induce blood vessel growth, or choroidal neovascularization (CNV), which mimics the human AMD pathology. Recombinant, mature IL-18 injected into the eyes of mice or subcutaneously limited CNV formation. It has been suggested that IL-18 is toxic, but Doyle *et al.* showed that this is not the case through in vitro and in vivo studies; the "pro" form of the cytokine is, however, and can be regulated by autophagy. Because IL-18 is being tested in patients with cancer, the authors believe that this could translate and readily complement existing antiangiogenic strategies currently used for AMD, such as the antibody-based therapies targeting vascular endothelial growth factor (VEGF).

Science Translational Medicine (print ISSN 1946-6234; online ISSN 1946-6242) is published weekly, except the last week in December, by the American Association for the Advancement of Science, 1200 New York Avenue, NW, Washington, DC 20005.

Science Translational Medicine (print ISSN 1946-6234; online ISSN 1946-6242) is published weekly, except the last week in December, by the American Association for the Advancement of Science, 1200 New York Avenue, NW, Washington, DC 20005.